

Properties of Hepatitis Delta Virus Ribozyme, Which Consists of Three RNA Oligomer Strands¹

Taiichi Sakamoto, Yoichiro Tanaka, Tomoko Kuwabara, Mi Hee Kim, Yasuyuki Kurihara, Masato Katahira, and Seiichi Uesugi²

Department of Bioengineering, Faculty of Engineering, Yokohama National University, 79-5 Tokiwadai, Hodogaya-ku, Yokohama 240

Received for publication, January 28, 1997

Properties of a hepatitis delta virus (HDV) RNA ribozyme system, which consists of three RNA oligomer strands (substrate 8-mer; enzyme 16-mer plus 35-mer) and contains a hybrid sequence of genomic and antigenomic RNA cores, are reported. Effects of Mg^{2+} concentration, divalent metal ion species, pH, and temperature on the cleavage activity were examined. The substrate cleavage activity increased with increasing Mg^{2+} concentration (0–100 mM). Ca^{2+} and Mn^{2+} ions were the most effective divalent cations and Mg^{2+} was less effective. The cleavage activity increased with increasing pH (5–7.5). The optimum temperature for the cleavage activity was 25–40°C. The Mg^{2+} concentration, pH and temperature dependencies are different from those reported for the single-strand ribozymes (about 90-mer) although the divalent metal ion preference is very similar. Conformational change induced by Mg^{2+} ion titration was monitored by CD. The CD data and the activity- Mg^{2+} concentration data were analyzed by curve-fitting analysis using equations derived for multiple metal ion binding mechanisms. The data can be explained by a model in which three Mg^{2+} ions bind to one ribozyme unit.

Key words: hepatitis delta virus, metal binding, oligonucleotide, ribozyme, RNA.

Human hepatitis delta virus (HDV) is a satellite virus which infects specifically cells already infected with hepatitis B virus. The HDV genome consists of a circular, single-strand RNA of about 1,700 nucleotides in length (1). The genome is replicated by the rolling circle mechanism (2, 3) and self-cleavage reactions of polymeric forms of antigenomic and genomic RNAs are involved in the process (2–4), as in the case of plant-pathogenic RNAs such as viroid and virusoid. The cleavage reaction of the HDV ribozyme requires divalent metal cations and produces RNA fragments with 2',3'-cyclic phosphate and 5'-hydroxyl groups by transesterification (2, 3), as in the case of the hammerhead ribozyme and hairpin ribozyme found in the plant pathogens.

The nucleotide sequence required for the cleavage activity of HDV ribozyme is very different from those of the other ribozymes, in spite of the similarity in the cleavage reaction schemes. Some models for the secondary folding structure of the catalytic core were proposed (5–11) and

experiments involving mutagenesis (12–14), chemical modification (15), and limited digestion by specific nucleases (8, 14) were done to find the answer. Most of the results support the "pseudoknot" structure model proposed by Perrotta and Been (7). The pseudoknot secondary structure model for the essential part of HDV ribozyme contains four double-stranded stems (P1–P4), a hairpin loop (L3), and two internal loops (J1/2 and J4/2) (4) (Fig. 1).

For structural study of HDV ribozyme by NMR, it is highly desirable to have a ribozyme system as small as possible to simplify the spectrum. Moreover, the system should be divided into fragments, since partial labeling of each fragment with stable isotopes such as ^{13}C and ^{15}N is usually necessary for signal assignment. For this purpose, we designed an HDV ribozyme system which consists of three RNA oligomer strands: substrate 8-mer and enzyme, 16-mer plus 35-mer; total length, 59 nucleotides. We synthesized the RNA oligomers and examined the properties of the ribozyme system. It turned out that this system has an activity comparable to that of larger ribozymes, which consist of one or two RNA strands, at high Mg^{2+} concentration and has similar divalent metal specificity. The dissociation constants and number of Mg^{2+} ions bound in the Mg^{2+} -ribozyme complex were estimated from curve-fitting analysis of the Mg^{2+} dependencies of the activity and conformation of the complex.

MATERIALS AND METHODS

Preparation of HDV Ribozyme—All solutions except for

¹ This research was supported in part by Grants-in-Aid for Scientific Research on Priority Areas (#05265211, #05244101, #06276103, #08249212, #08680715) from the Ministry of Education, Science, Sports and Culture of Japan and by the Proposal-Based Advanced Industrial Technology R&D Program from the New Energy and Industrial Technology Development Organization (NEDO) of Japan. M.K. was supported by grants from the Kanagawa Academy of Science and Technology and Kato Memorial Bioscience Foundation.

² To whom correspondence should be addressed. Phone/Fax: +81-45-339-4265, E-mail: uesugi@mac.bio.bsk.ynu.ac.jp
Abbreviations: HDV, hepatitis δ virus; MES, 2-(*N*-morpholino)-ethanesulfonic acid; NTP, ribonucleoside triphosphate; PEI, poly(ethylenimine); PEG, polyethylene glycol; Rz, ribozyme.

Tris-HCl buffer were treated with diethyl pyrocarbonate and autoclaved to inactivate a trace of ribonucleases. The substrate RNA 8-mer was chemically synthesized and supplied by Genset. It was purified by denaturing (7 M urea) polyacrylamide gel electrophoresis. The gel containing the 8-mer was crushed and soaked overnight in 0.3 M sodium acetate (pH 7) with shaking at room temperature. The extracted RNA was isolated by two rounds of ethanol precipitation at -25°C for 2 h. The enzyme components, RNA 16-mer and 35-mer, were prepared by *in vitro* transcription with T7 RNA polymerase using fully double-stranded DNA promoter-template. T7 RNA polymerase was prepared by overexpression of its gene in *Escherichia coli* BL21 carrying the plasmid pAR1219 (16). The DNA oligomers, 32-mers and 51-mers, for the promoter-template DNAs, were synthesized with a DNA synthesizer (model 392, Applied Biosystems) and purified in the same manner as described for the substrate RNA oligomer. Transcription reaction was carried out at 37°C for 6 h according to the procedure of Milligan *et al.* (17) with some modifications. The reaction mixture (200 μl) contained the promoter-template DNA (2 μM), T7 RNA polymerase (0.1 mg/ml), 4 ribonucleoside triphosphates (7.5 mM each), MgCl_2 (35 mM), Tris-HCl (pH 8.1, 40 mM), DTT (5 mM), spermidine (70 mM), Triton X-100 (0.1%, v/v), and PEG8000 (80 mg/ml). The RNA oligomers were identified by sequence determination. The oligomers were labeled at the 5'-ends by using polynucleotide kinase (Takara Shuzo) and [γ - ^{32}P]ATP (about 6,000 Ci/mmol) after dephosphorylation with alkaline phosphatase (Takara Shuzo) when necessary. The labeled RNA was subjected to partial alkaline hydrolysis (18) and partial digestion with RNase T1, RNase U2, RNase phyM, and *Bacillus cereus* RNase (Pharmacia). The degradation products were separated by denaturing 20% polyacrylamide gel electrophoresis and the sequence was determined by comparison of the product bands. Yield and concentration of RNA oligomers were calculated from absorbance at 260 nm using the molar absorption coefficients of the component nucleotides.

Measurement of CD Spectra—CD spectra were measured on a J-720 spectropolarimeter (JASCO, Tokyo). The Mg^{2+} titration experiment was performed in a 10-mm cell with the HDV ribozyme complex (1 μM) containing non-cleavable substrate in 10 mM sodium phosphate buffer (pH 7.0) at 37°C . A mixture of the RNA oligomers (1 μM each) in the buffer (300 μl) was annealed by heating at 90°C for 3 min and gradual cooling to room temperature. CD spectra were scanned four times for each sample, averaged, and smoothed using software provided by JASCO. The Mg^{2+} concentration was varied by addition of concentrated MgCl_2 solution.

CD-temperature profiles were obtained with the ribozyme complex (1 μM) containing the non-cleavable substrate in 10 mM sodium phosphate buffer (pH 7.0) with or without 10 mM MgCl_2 . The sample was annealed in the same manner as described above and cooled to 5°C before measurement. Then the temperature of the sample was raised from 5 to 80°C at a rate of $50^{\circ}\text{C}/\text{h}$ with monitoring of the ellipticity at 265 nm.

Substrate RNA Cleavage Reaction—To determine the pseudo first-order rate constant (k_{obs}) of the substrate RNA cleavage reaction and to find the lowest suitable substrate to enzyme ratio, the cleavage reactions were tried at

various values of the substrate to enzyme ratio (1–1,000). The 5'-labeled substrate (0.1 μM) and the enzyme components (0.1–100 μM) were dissolved in 50 mM Tris-HCl (pH 8), heated at 90°C for 3 min and cooled gradually to room temperature. MgCl_2 (final concentration, 10 mM) was added to the solution to start the reaction and the mixture was incubated at 37°C . Aliquots of the mixture were withdrawn during the reaction time (up to 24 h) and the reaction was stopped by addition of 2 volumes of 50 mM EDTA. The reaction mixture was applied on a thin-layer plate of PEI-cellulose. The plate was developed first with water, then dried and developed with 1 M LiCl to separate the product (pC>p) from the substrate 8-mer (19). Radioactivity of the spots was quantitated using a Bioimage Analyzer (BAS2000, Fuji Film). The k_{obs} values were calculated by curve-fitting analysis of the cleavage yield (P) vs. time (t) data using the equation $P = P_{\text{max}} [1 - \exp(-k_{\text{obs}}t)]$; P_{max} : the cleavage yield at infinite time (usually $P_{\text{max}} = 0.8$ – 0.9). The effects of Mg^{2+} concentration, metal ion species, pH, and temperature on the cleavage activity were also examined in reactions with the substrate (0.1 μM) and the enzyme (1 μM). The reaction conditions were the same as described above except for each varied factor, as shown in the figure legends.

RESULTS AND DISCUSSION

Design and Synthesis of RNAs—The designed ribozyme system consists of three RNA strands (Fig. 1c). The RNA chain of the original single-strand ribozyme system is broken at two regions, at the junction J1/2 and in the middle of the long stem P4 (Fig. 1a). The substrate component is an 8-mer and contains only one nucleotide residue on the 5'-side of the scissile bond (20). The enzyme component consists of a 16-mer and a 35-mer. The sequences of this system are a hybrid of genomic (a part of P2 and J4/2) and antigenomic (P1, L3, and P4) sequences and are essentially the same as those designed by Been *et al.* for a two-strand system (12). The total chain length of this system is 59 nucleotide units; this is the smallest HDV ribozyme system reported so far.

The RNA oligomer for the substrate 8-mer was chemically synthesized because it lacks the 5'-terminal G residue which is required for efficient enzymatic synthesis. The RNA oligomers for the enzyme component, 16-mer and 35-mer, were prepared by using T7 RNA polymerase: 5 nmol of 16-mer (turnover number, 10) and 7.5 nmol of 35-mer (turnover number, 15) were obtained from a reaction on a 200- μl scale. The base sequences of these oligomers and the substrate 8-mer were confirmed by RNA sequence analysis using alkaline hydrolysis and digestion with specific nucleases (data not shown).

Effect of Enzyme Concentration on the Cleavage Rate—To determine the single-turnover rate constant at a saturating concentration of the enzyme for the substrate, the cleavage reactions were performed with the substrate (0.1 μM) and the enzyme (0.1–100 μM) at 37°C and pH 8 in the presence of 10 mM MgCl_2 . The k_{obs} vs. enzyme concentration profile is shown in Fig. 2. A maximum k_{obs} ($\sim 0.09 \text{ min}^{-1}$) was observed at around 1–5 μM enzyme (enzyme/substrate ratio, 10–50). The cleavage activity decreases at higher enzyme concentration (over 10 μM). The decrease may be due to self-association of the enzyme component(s)

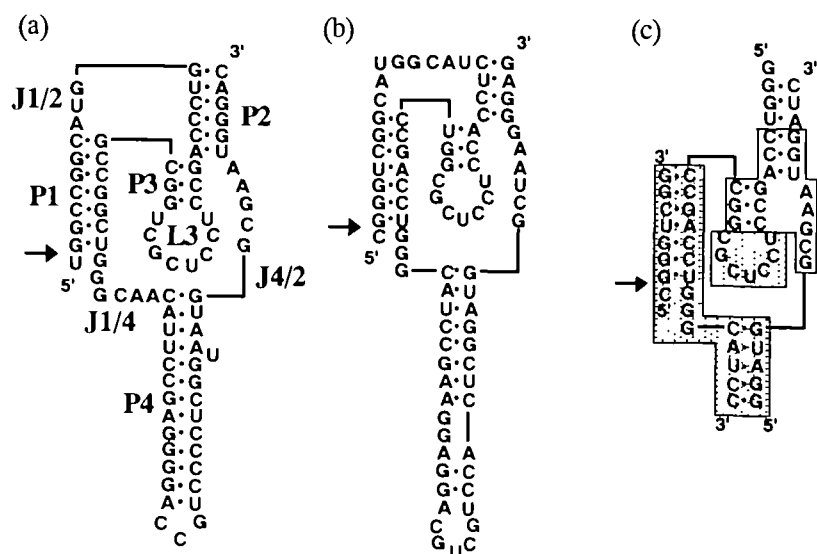


Fig. 1. Nucleotide sequences and possible secondary structures of HDV ribozymes. (a) the genomic sequence, (b) the antigenomic sequence, (c) designed mutant ribozyme with a hybrid sequence where the genomic sequence is shown in a box and the antigenomic sequence is shown in stippled boxes. Arrows indicate the sites of cleavage.

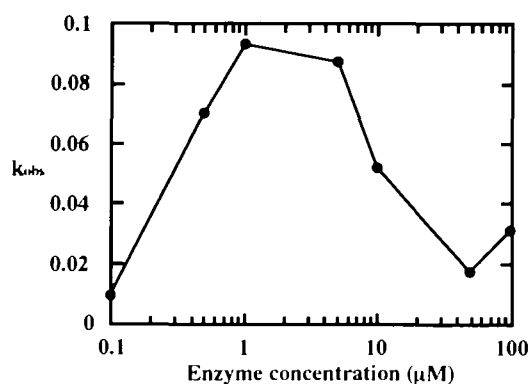


Fig. 2. Dependence of cleavage rate on enzyme concentration under conditions of single turnover. The cleavage reaction was carried out with the substrate ($0.1 \mu\text{M}$) and various concentration of the enzyme ($0.1\text{--}100 \mu\text{M}$) in 50 mM Tris-HCl (pH 8), 10 mM MgCl_2 at 37°C .

preventing proper enzyme complex formation. All the cleavage reactions examined thereafter were performed with the substrate ($0.1 \mu\text{M}$) and the enzyme ($1 \mu\text{M}$).

Effect of Mg^{2+} Concentration on the Cleavage Activity—The effect of Mg^{2+} concentration ($0\text{--}100 \text{ mM}$) on the cleavage activity was examined at 37°C and pH 8. The k_{obs} vs. Mg^{2+} concentration profile is shown in Fig. 3. The cleavage rate increases with increasing Mg^{2+} concentration ($0\text{--}100 \text{ mM}$). The k_{obs} at 100 mM Mg^{2+} (0.38 min^{-1}) is about 4 times as high as that at 10 mM Mg^{2+} (0.09 min^{-1}). The k_{obs} value at 100 mM MgCl_2 is comparable to those (1.5 and 0.52 min^{-1}) reported for two-strand HDV ribozymes with similar sequences in the presence of 10 mM MgCl_2 at 37°C (12). It is reported that the cleavage yield after 1 h for single-strand HDV ribozymes (101-mer and 91-mer) increases with increasing Mg^{2+} concentration, but reaches a plateau at around 1 mM Mg^{2+} (21). It seems that our three-strand ribozyme has lower affinity for Mg^{2+} ions. Although the cleavage rate is higher at 100 mM MgCl_2 , further experiments were carried out at 10 mM MgCl_2 since around 10 mM MgCl_2 is usually employed as the standard reaction condition (12, 22, 25) and the cleavage

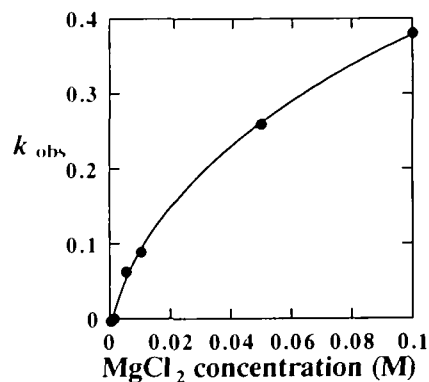


Fig. 3. Dependence of cleavage rate on MgCl_2 concentration. The reaction was carried out with the substrate ($0.1 \mu\text{M}$), the enzyme ($1 \mu\text{M}$) and various concentrations of MgCl_2 ($0\text{--}100 \text{ mM}$) in 50 mM Tris-HCl (pH 8) at 37°C . The best-fit curve calculated for the three- Mg^{2+} ion binding model is shown by a solid line.

rate is appropriate for experimental convenience.

The Effect of Other Metal Ions on the Cleavage Activity—The effects of divalent metal ions (10 mM) other than Mg^{2+} were examined at pH 7.0, and the cleavage yields after 5 min were compared (Table I). The reaction with CaCl_2 gave the highest yield, about 3-fold higher than that with MgCl_2 . MnCl_2 showed activity comparable to that for Ca^{2+} . The reaction with ZnCl_2 or CoCl_2 gave a poor yield, about one-tenth of that in the case of Mg^{2+} . These results are similar to those reported for the single-strand ribozymes (21), where Mn^{2+} , Mg^{2+} , and Ca^{2+} show comparable activity for supporting the cleavage reaction. It is rather surprising that 10 mM Ca^{2+} is much more effective than 10 mM Mg^{2+} in the case of the three-strand ribozyme system.

Effect of pH on the Cleavage Activity—To examine the effect of pH, the cleavage reactions were carried out with 10 mM Mg^{2+} at various values of pH ($5\text{--}8$) at 37°C for 5 min (Fig. 4). The cleavage yield increases with increasing pH in the pH range of $6\text{--}7.5$. This result is very similar to that observed for hammerhead ribozymes, suggesting that some deprotonation process enhances the cleavage rate. The result is very different from that reported for single-strand

TABLE I. Effects of metal cation species on the cleavage yield. The cleavage reaction was carried out with the substrate (0.1 μ M), the enzyme (1 μ M) and 10 mM metal chloride in 50 mM Tris-HCl buffer (pH 7) at 37°C for 5 min.

Metal chloride	Cleavage yield (%)
MgCl ₂	22
MnCl ₂	56
CaCl ₂	66
ZnCl ₂	3
CoCl ₂	2

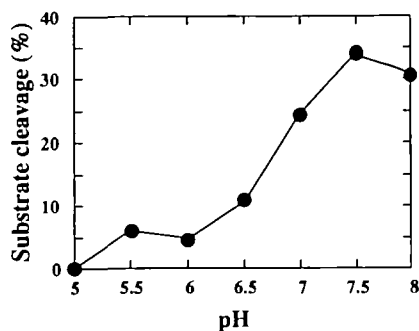


Fig. 4. Dependence of cleavage yield on pH. The reaction was carried out with the substrate (0.1 μ M) and the enzyme (1 μ M) in 10 mM MgCl₂ and 50 mM buffer (pH 5–6.5, MES buffer; pH 7–8, Tris buffer) at 37°C for 5 min.

HDV ribozymes (88–194-mer), where a higher cleavage yield is observed at acidic pH (5–6) than that at pH 7–9 (22).

Effect of Temperature on the Cleavage Activity—To examine the effect of temperature, the cleavage reactions were carried out with 10 mM Mg²⁺ at various temperatures (5–60°C) and pH 8 for 5 min (Fig. 5). The optimum temperature was around 25–40°C. The substrate-enzyme complex (1 μ M), which contained a non-cleavable substrate with 2'-O-methylcytidine at the cleavage site, showed T_m at around 63°C in the presence of 10 mM MgCl₂ at pH 8 as monitored by CD spectroscopy, while the complex showed T_m at around 22 and 48°C in the absence of Mg²⁺ ions (data not shown). These results suggest that the HDV ribozyme complex takes a fully folded conformation which is active for catalysis in the optimum temperature range under the cleavage reaction conditions. In the case of other HDV ribozyme systems, which are single-strand systems (90-mer and 117-mer), much higher optimum temperatures (around 60 and 70°C, respectively) have been reported (22, 23).

Effect of Mg²⁺ Concentration on the Conformation—To examine conformational change induced by addition of Mg²⁺, CD spectra of the HDV ribozyme complex (1 μ M) were measured at various MgCl₂ concentrations (0–77 mM) and 37°C (Fig. 6a). The CD spectra show a positive band at around 270 nm. The intensity of this band increases with increasing Mg²⁺ concentration. The profile of normalized CD intensity increase at 265 nm *vs.* Mg²⁺ concentration is shown in Fig. 6b. The CD change is assumed to reflect the conformational change in the complex induced by Mg²⁺ ion binding. Therefore, the normalized CD change may correspond to the fraction (f) of Mg²⁺-bound complex. The profile suggests that the complex is almost saturated with

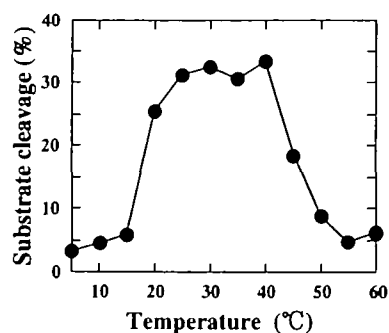


Fig. 5. Dependence of cleavage yield on temperature. The reaction was carried out with the substrate (0.1 μ M) and the enzyme (1 μ M) in 50 mM Tris buffer (pH 8), 10 mM MgCl₂ for 5 min at various temperatures (5–60°C).

Mg²⁺ ions at 20 mM MgCl₂. This profile is very different from that of cleavage rate *vs.* Mg²⁺ concentration. If only one Mg²⁺ ion binds to the complex, these two profiles should be similar because k_{obs} is proportional to the fraction of Mg²⁺-bound complex. Therefore, the present results suggest that the number of Mg²⁺ ion bound to the complex is more than one.

Analysis of the Number of Mg²⁺ Ions Bound to a Ribozyme—For interactions involving a ribozyme (Rz) and two Mg²⁺ ions, the following equations can be written:

$$K_{a1} = [\text{Rz-Mg}^{2+}] / [\text{Rz}][\text{Mg}^{2+}]$$

$$K_{a2} = [\text{Rz-2Mg}^{2+}] / [\text{Rz-Mg}^{2+}][\text{Mg}^{2+}]$$

$$F_1 = [\text{Rz-Mg}^{2+}] / ([\text{Rz}] + [\text{Rz-Mg}^{2+}] + [\text{Rz-2Mg}^{2+}])$$

$$F_2 = [\text{Rz-2Mg}^{2+}] / ([\text{Rz}] + [\text{Rz-Mg}^{2+}] + [\text{Rz-2Mg}^{2+}])$$

From these equations, we can derive the following relations.

$$F_1 = K_{a1}[\text{Mg}^{2+}] / (1 + K_{a1}[\text{Mg}^{2+}] + K_{a1}K_{a2}[\text{Mg}^{2+}]^2)$$

$$F_2 = K_{a1}K_{a2}[\text{Mg}^{2+}]^2 / (1 + K_{a1}[\text{Mg}^{2+}] + K_{a1}K_{a2}[\text{Mg}^{2+}]^2)$$

For interactions involving a ribozyme and three Mg²⁺ ions, the following relations can be derived in the similar manner.

$$F_1 = K_{a1}[\text{Mg}^{2+}] / (1 + K_{a1}[\text{Mg}^{2+}] + K_{a1}K_{a2}[\text{Mg}^{2+}]^2 + K_{a1}K_{a2}K_{a3}[\text{Mg}^{2+}]^3)$$

$$F_2 = K_{a1}K_{a2}[\text{Mg}^{2+}]^2 / (1 + K_{a1}[\text{Mg}^{2+}] + K_{a1}K_{a2}[\text{Mg}^{2+}]^2 + K_{a1}K_{a2}K_{a3}[\text{Mg}^{2+}]^3)$$

$$F_3 = K_{a1}K_{a2}K_{a3}[\text{Mg}^{2+}]^3 / (1 + K_{a1}[\text{Mg}^{2+}] + K_{a1}K_{a2}[\text{Mg}^{2+}]^2 + K_{a1}K_{a2}K_{a3}[\text{Mg}^{2+}]^3)$$

In the present system where the total concentration of ribozyme is negligibly low with respect to the concentration of added MgCl₂, the concentration of free Mg²⁺ ([Mg²⁺]) is essentially equal to the total concentration of Mg²⁺.

In the case of the two-Mg²⁺ ion binding model, when the contribution of $[\theta]$ change from the Rz-Mg²⁺ species relative to that from Rz-2Mg²⁺ is r_1 , the normalized $[\theta]$ change, F_{cd} , can be described as follows:

$$F_{cd} = r_1 F_1 + F_2$$

Similarly, F_{cd} for the three-Mg²⁺ ion binding model can be described as follows:

$$F_{cd} = r_1 F_1 + r_2 F_2 + F_3$$

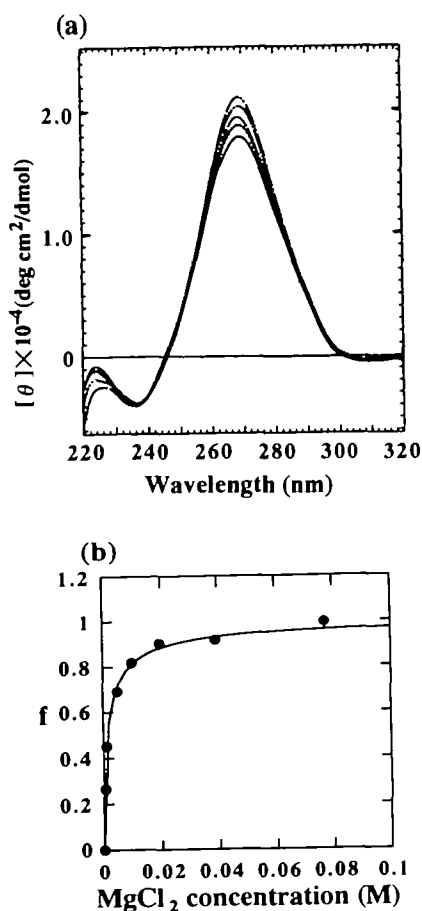


Fig. 6. Effect of Mg^{2+} concentration on CD spectra of the ribozyme complex. (a) CD spectra for the HDV ribozyme complex ($1 \mu\text{M}$) containing non-cleavable substrate in 10 mM sodium phosphate buffer (pH 7) containing 0 mM (—), 0.5 mM (.....), 1 mM (---), 5 mM (-·-·-), and 10 mM MgCl_2 (- - - -) at 37°C. (b) Normalized $[\theta]_{265}$ increase (f) induced by Mg^{2+} addition was plotted against MgCl_2 concentration. The best-fit curve calculated for the three- Mg^{2+} ion binding model is shown by a solid line.

Curve-fitting analysis of the experimental data using the nonlinear least-squares method gave the following parameters: $K_{d1}=0.74$ mM, $K_{d2}=10$ mM, $r_1=0.68$ for the two- Mg^{2+} binding model; $K_{d1}=0.70$ mM, $K_{d2}=8.0$ mM, $K_{d3}=164$ mM, $r_1=0.65$, $r_2=0.97$ for the three- Mg^{2+} binding model (K_a is converted to K_d by using the relation: $K_d=1/K_a$). Thus, the CD data can be explained by both models. When the activity data (k_{obs} vs. $[\text{Mg}^{2+}]$) data were analyzed by curve-fitting using a similar equation, $k_{obs}=a(r'_1F_1+F_2)$ or $k_{obs}=a(r'_1F_1+r'_2F_2+F_3)$ where a is a factor for calculating k_{obs} , and the K_a values obtained above, the parameters from the three- Mg^{2+} ion model gave a better fit with a parameter set: $a=0.81$, $r'_1=0.0$ and $r'_2=0.17$. These r' values imply that the Rz-Mg^{2+} species makes a very small contribution to the activity and the Rz-2Mg^{2+} species is about 6-fold less active than the Rz-3Mg^{2+} species.

The curve-fitting technique was also applied directly to the activity data. The three- Mg^{2+} binding model again gave a better fit than the two- Mg^{2+} binding model with a parameter set: $a=0.81$, $r'_1=0.0$, $r'_2=0.14$, $K_{d1}=0.76$ mM, $K_{d2}=6.0$ mM, $K_{d3}=156$ mM. These values are

almost the same as those obtained from the analysis of the CD data. These results described above reveal that the three- Mg^{2+} ion binding model can explain the Mg^{2+} -concentration-dependent changes of both conformation and activity of the HDV ribozyme.

CONCLUSIONS

The three-strand HDV ribozyme system (total length, 59 nucleotides) described in this paper is the smallest system reported so far. This system showed a selectivity for divalent cations (high preference for Ca^{2+} , Mn^{2+} , and Mg^{2+}) similar to that of single-strand HDV ribozyme systems (101- and 91-mers with the genomic sequence) (21). This system differs in some properties from other HDV ribozyme systems, which comprise one or two strands and are larger in terms of total chain length, *i.e.*, the dependence of the cleavage activity on pH and temperature are different. In the present system, the cleavage activity increases with increasing pH in the range of 6–7.5 and shows an optimum temperature of around 25–40°C, whereas some other ribozymes show higher activity in the acidic region than at neutral pH (22) and show much higher optimum temperature (22, 23). It has also been reported that addition of denaturing agents such as formamide and urea enhances the cleavage reaction for some larger HDV ribozyme systems (22, 24, 25), while addition of 5 M urea markedly reduced the cleavage yield for the present system (Sakamoto, unpublished data). These phenomena can be explained by the idea that the larger ribozymes take on an inactive conformation at low temperature and neutral pH, and undergo conformational conversion to an active form upon acidification, raising the temperature or adding denaturing agents. The present system may be small enough to take on an active form at lower temperature because it lacks unnecessary flanking sequences which may interact with the catalytic core sequence to form an inactive folding conformation. This is an excellent feature of this system for studies on the mechanism of HDV ribozyme catalysis, as well as for elucidation of the active structure.

Curve-fitting analysis of the CD- Mg^{2+} concentration data revealed that the CD data can be explained by a two- Mg^{2+} ion binding model or a three- Mg^{2+} ion binding model. However, the parameter set obtained from the three- Mg^{2+} binding model gave a better fit for the cleavage rate- Mg^{2+} concentration data. When the activity data were directly analyzed by curve-fitting, the three- Mg^{2+} ion binding model again gave the best-fit parameters, which are almost the same as those obtained from the CD data. The parameters for the activity data ($r'_1=0.0$ and $r'_2=0.17$) suggest that of the three Mg^{2+} ions bound to the ribozyme, two mainly contribute to the catalytic activity. The number of Mg^{2+} ions bound to the ribozyme is similar to that obtained for hammerhead ribozymes by curve-fitting analysis of the CD and activity data (26); the two- Mg^{2+} ion binding gives the best-fit curve for a two-strand hammerhead ribozyme mutant with deletion of stem II and three or more Mg^{2+} ions are assumed to be involved in the case of a three-strand hammerhead ribozyme. In the case of the hammerhead ribozymes, it is assumed that at least two Mg^{2+} ions are involved in catalysis from kinetic studies (27). Considering the similarity of the chemical process in RNA cleavage between hammerhead and HDV ribozymes, it is very likely

that two or more Mg^{2+} ions are also involved in the catalysis of HDV ribozymes. At present, it is not known whether the three- Mg^{2+} binding model might be applicable to other single-strand or two-strand HDV ribozyme systems, since k_{obs} vs. Mg^{2+} concentration profiles have not been reported. Cleavage yield vs. Mg^{2+} concentration data (21, 22, 24) for single-strand HDV ribozymes only suggest that they may have smaller K_d s.

We thank Dr. F.W. Studier for providing us with the strain BL21 containing plasmid pAR1219.

REFERENCES

- Taylor, J. (1991) Hepatitis delta virus. *J. Hepatol.* **13**, s114-s115
- Kuo, M.Y.P., Sharmeen, L., Dinter-Gottlieb, G., and Taylor, J. (1988) Characterization of self-cleaving RNA sequences on the genome and antigenome of human hepatitis delta virus. *J. Virol.* **62**, 4439-4444
- Sharmeen, L., Kuo, M.Y.P., Dinter-Gottlieb, G., and Taylor, J. (1988) Antigenomic RNA of human hepatitis delta virus can undergo self-cleavage. *J. Virol.* **62**, 2674-2679
- Been, M.D. (1994) *Cis*- and *trans*-acting ribozymes from a human pathogen, hepatitis delta virus. *Trends Biochem. Sci.* **19**, 251-256
- Wu, H.-N., Lin, Y.-J., Lin, F.-P., Makino, S., Chang, M.-F., and Lai, M.M.C. (1989) Human hepatitis δ virus RNA subfragments contain an autocleavage activity. *Proc. Natl. Acad. Sci. USA* **86**, 1831-1835
- Wu, H.-N., Wang, Y.-J., Hung, C.-F., Lee, H.-J., and Lai, M.M.C. (1992) Sequence and structure of the catalytic RNA of hepatitis delta virus genomic RNA. *J. Mol. Biol.* **223**, 233-245
- Perrotta, A.T. and Been, M.D. (1991) A pseudoknot-like structure required for efficient self-cleavage of hepatitis delta virus RNA. *Nature* **350**, 434-436
- Rosenstein, S.P. and Been, M.D. (1991) Evidence that genomic and antigenomic RNA self-cleaving elements from hepatitis delta virus have similar secondary structures. *Nucleic Acids Res.* **19**, 5409-5416
- Belinsky, M. and Dinter-Gottlieb, G. (1991) Non-ribozyme sequences enhance self-cleavage of ribozymes derived from hepatitis delta virus. *Nucleic Acids Res.* **19**, 559-564
- Branch, A. and Robertson, H.D. (1991) Efficient *trans* cleavage and a common structural motif for the ribozymes of the human hepatitis δ agent. *Proc. Natl. Acad. Sci. USA* **88**, 10163-10167
- Thill, G., Blumenfeld, M., Lescure, F., and Vasseur, M. (1991) Self-cleavage of a 71 nucleotide-long ribozyme derived from hepatitis delta virus genomic RNA. *Nucleic Acids Res.* **19**, 6519-6525
- Been, M.D., Perrotta, A.T., and Rosenstein, S.P. (1992) Secondary structure of the self-cleaving RNA of hepatitis delta virus: Applications to catalytic RNA design. *Biochemistry* **31**, 11843-11852
- Perrotta, A.T. and Been, M.D. (1993) Assessment of disparate structural features in three models of the hepatitis delta virus ribozyme. *Nucleic Acids Res.* **21**, 3959-3965
- Perrotta, A.T., Rosenstein, S.P., and Been, M.D. (1993) Experimental evidence for the secondary structure of the hepatitis delta virus ribozyme. *Prog. Clin. Biol. Res.* **382**, 69-77
- Kumar, P.K.R., Taira, K., and Nishikawa, S. (1994) Chemical probing studies of the variants of the genomic hepatitis delta virus ribozyme by primer extension analysis. *Biochemistry* **33**, 583-592
- Davanloo, P., Rosenburg, A.H., Dunn, J.J., and Studier, F.W. (1984) Cloning and expression of the gene for bacteriophage T7 RNA polymerase. *Proc. Natl. Acad. Sci. USA* **81**, 2035-2039
- Milligan, J.F., Groebe, D.R., Witherell, G.W., and Uhlenbeck, O.C. (1987) Oligoribonucleotide synthesis using T7 RNA polymerase and synthetic DNA template. *Nucleic Acids Res.* **15**, 8783-8798
- Kuchino, Y. and Nishimura, S. (1989) Enzymatic RNA sequencing in *Methods in Enzymology* (Dahlberg, J.E. and Abelson, J.N., eds.) Vol. 180, pp. 154-163, Academic Press, New York
- Perrotta, A.T. and Been, M.D. (1992) Cleavage of oligoribonucleotides by a ribozyme derived from the hepatitis δ virus RNA sequence. *Biochemistry* **31**, 16-21
- Tanner, N.K., Schaff, S., Thill, G., Petit-Koskas, E., Crain-Denoyelle, A.-M., and Westhof, E. (1994) A three-dimensional model of hepatitis delta virus ribozyme based on biochemical and mutational analyses. *Curr. Biol.* **4**, 488-498
- Suh, Y.-A., Kumar, P.K.R., Taira, K., and Nishikawa, S. (1993) Self-cleavage activity of the genomic HDV ribozyme in the presence of various divalent metal ions. *Nucleic Acids Res.* **21**, 3277-3280
- Wu, H.-N. and Lai, M.M.C. (1990) RNA conformational requirements of self-cleavage of hepatitis delta virus RNA. *Mol. Cell. Biol.* **10**, 5575-5579
- Thill, G., Vasseur, M., and Tanner, N.K. (1993) Structural and sequence elements required for the self-cleaving activity of the hepatitis delta virus ribozyme. *Biochemistry* **32**, 4254-4262
- Rosenstein, S.P. and Been, M.D. (1990) Self-cleavage of hepatitis delta virus genomic strand RNA is enhanced under partially denaturing conditions. *Biochemistry* **29**, 8011-8016
- Smith, J.B. and Dinter-Gottlieb, G. (1991) Antigenomic hepatitis delta virus ribozymes self-cleave in 18 M formamide. *Nucleic Acids Res.* **19**, 1285-1289
- Sakamoto, T., Kim, M.H., Kurihara, Y., Sasaki, N., Noguchi, T., Katahira, M., and Uesugi, S. (1997) Properties of a hammerhead ribozyme with deletion of stem II. *J. Biochem.* **121**, 288-294
- Sawata, S., Komiyama, M., and Taira, K. (1995) Kinetic evidence based on solvent isotope effects for the nonexistence of a proton-transfer process in reactions catalyzed by a hammerhead ribozyme: Implication to the double-metal-ion mechanism of catalysis. *J. Am. Chem. Soc.* **117**, 2357-2358